Review

Improved pressure decay method for measuring CO₂-water diffusion coefficient without convection interference

Enoc Basilio [a], Mouadh Addassi [a], Mohammed Al-Juaied [a], S. Majid Hassanizadeh [b,c], Hussein Hoteit [a,*]

[a] *King Abdullah University of Science and Technology (KAUST), Thuwal 23955, Saudi Arabia*
[b] *Stuttgart Center for Simulation Science, Stuttgart University, Germany*
[c] *Department of Earth Sciences, Utrecht University, the Netherlands*

ARTICLE INFO

ABSTRACT

Carbon dioxide (CO_2) storage in deep aquifers is a promising solution to mitigate anthropogenic CO_2 emissions. CO_2 solubility in brine results in a non-buoyant phase providing an effective trapping mechanism. However, experimental work and numerical simulation results have shown that this diffusion-driven mechanism is a relatively slow process. Accurate determination of CO_2 diffusion coefficient is, therefore, essential. The pressure decay method is a widely employed technique for measuring diffusion coefficients of gases in bulk liquids or porous media. It involves introducing a volume of gas on top of the liquid in a closed system and monitoring the pressure decay over time. While the method is generally simple and accurate, artifacts from natural convection can significantly influence the measured diffusion for liquids that exhibit an increase in density due to gas dissolution. This work presents an improved experimental approach for measuring CO_2 diffusion coefficients in water in a convection-fee system. Our setup consisted of single open-ended borosilicate capillary tubes filled with water inside a high-pressure vessel filled with CO_2 gas. The water-filled capillary tubes were placed with their open ends facing down. This configuration exhibits bottom-top diffusion leading to gravity-stable CO_2 diffusion in water free of gravity-induced convection and viscous fingering. The effects of pressure and salinity variations confirm the agreement between our results and values reported in the literature. We also performed additional analysis to determine the effective diffusion coefficient of CO_2 in a porous medium. The proposed technique can be used to measure the diffusion coefficients for other gas-liquid systems.

1. Introduction

There is a general consensus in the scientific community that global warming and climate change are being caused by anthropogenic emissions of carbon dioxide (CO_2) and other greenhouse gases worldwide. Among possible storage options, a viable alternative is offered by saline aquifers (Lackner, 2003), which are geological formations comprising permeable rocks saturated with brine. Saline aquifers provide large storage capacities (see Table 1) without impacting drinking or irrigation water resources (Firoozabadi and Myint, 2010). Previous studies suggest the best option is the injection of CO_2 in its supercritical phase (scCO₂) at the subsurface temperature and pressure conditions in deep saline aquifers (between 800- and 3000 m depth). Under those conditions, scCO₂ density varies between 266 and 766 kg/m³, and brine density varies between 945 and 1230 kg/m³ (Adams and Bachu, 2002;

Emami-Meybodi et al., 2015). This density difference leads to positive buoyancy for scCO₂, which results in gravity segregation and free-phase CO_2 cap formation in the upper part of the structure. Buoyant forces and injection pressure enhance the CO_2 upward movement, giving rise to a potential risk of leakage (Koide et al., 1992).

As the injected CO_2 column spreads and migrates upwards and laterally, part of the gas dissolves into the brine at the CO_2-brine interface. This results in a secure CO_2 trapping mechanism via a dissolution process referred to as solubility trapping (Addassi et al., 2022; Bachu and Adams, 2003; Oelkers et al., 2022; Spycher et al., 2003). CO_2 dissolution into the formation brine leads to some pressure decay in the free-phase CO_2, further lessening the risk of leakage. Density variations due to CO_2 dissolution have been reported to be 2 to 3 % heavier than pure water (Garcia, 2001) and 0.1 to 1 % heavier than brine solutions (Pruess and Zhang, 2008). This density difference results in an unstable boundary layer, starting an unstable density stratification and

---

* Corresponding author.
E-mail address: hussein.hoteit@kaust.edu.sa (H. Hoteit).

Nomenclature

c	molar concentration of gas in the liquid
c_s	concentration at the gas/liquid interface
D	molecular diffusion coefficient of gas in water
H	Henry's constant
l	height of the liquid column
M	molar mass of gas molecules
m	molal concentration
p_g	gas pressure in the vessel
p_i	initial gas pressure of the vessel
R_g	universal gas constant
t	time
T	system temperature
V_g	volume of gas
z	distance away from the interface
Z	gas compressibility factor

Special symbols

∂	partial differential operator
Δ	Difference operator

Subscripts

g	value in the gas phase
s	value under saturation condition

Table 1

Potential for subsurface CO_2 storage (Davison et al., 2001; Metz et al., 2005).

Storage Option	Global Capacity (Gt CO_2)
Depleted oil and gas fields	120–920
Deep saline reservoirs	100–10,000
Unmineable coal seams	3–200

eventually initiating Rayleigh-Bernard natural convection, also known as convective mixing. That is, denser CO_2-saturated brine sinks down from the interface due to gravity-driven convection while less dense brine rises upwards (Jafari Raad et al., 2016; Jafari Raad and Hassanzadeh, 2016; MacMinn et al., 2011; Macminn et al., 2010; Mohammadi et al., 2023; Yang et al., 2021). The gradual dissolution and spread of CO_2 into the brine column form a diffusive boundary layer that evolves with time (Lindeberg and Wessel-Berg, 1997). Convective mixing can significantly enhance the CO_2 dissolution rate. However, the spreading of dissolved CO_2 into the brine column below the convective mixing zone is a relatively slow process, limited by cross-phase molecular diffusion (Hoteit, 2013; Hoteit and Firoozabadi, 2018, 2009).

Assessing the interplay of dissolution and diffusion and evaluating the effective rate is paramount in calculating the transient effect of solubility. Obtaining experimental data on CO_2 diffusion coefficient as well as quantifying the effects of convection and diffusion mechanisms, are necessary for designing, optimizing, and monitoring CCS projects (Alqahtani et al., 2023; Omar et al., 2021). Depending on the properties of the host rock, the dissolution rate is controlled by either pure diffusion (in tight host rocks with low permeability) or convection-assisted diffusion. Experimental techniques for measuring molecular diffusion coefficients of liquid-gas binary systems, commonly classified as direct and indirect methods (Kantzas et al., 2022), have been extensively reported in the literature. Direct methods involve physicochemical techniques, where diffusion coefficients are estimated by compositional data analysis from direct measurements of gas/liquid mixture composition (Sigmund, 1976). They offer reliable results, isolating diffusion from

external phenomena (e.g., convective mixing). However, direct methods are usually more complex, expensive, time-consuming, and system-intrusive (Ghasemi et al., 2016; Mehrotra et al., 1987; Nguyen and Ali, 1998; Riazi and Whitson, 1993a; Sigmund, 1976). On the other hand, indirect methods rely on measuring diffusion coefficients by measuring other quantifiable parameters. There are two classes of indirect methods: (1) constant-volume methods (Ghasemi et al., 2016), where the rate of gas pressure decay in a confined system is measured and analyzed; (2) constant-pressure methods, in which gas pressure is kept constant across the gas-liquid interface by continuously supplying gas to the diffusion cell while the movement of gas-liquid interface and rate of gas injection are recorded and analyzed. However, Rayleigh-Bénard instabilities occur in most indirect methods, which lead to convective mixing and an accurate determination of molecular diffusion coefficient becomes difficult (Erfani et al., 2020; Getling, 2012; Ghorayeb and Firoozabadi, 2000). Various experimental techniques have been attempted by previous researchers to prevent convective mixing, including maintaining low system pressure and dividing the pressure decay curve into unsteady and steady stages and assuming that the steady stage is only governed by molecular diffusion (Ahmadi et al., 2020; Zhang et al., 2015; Zhao et al., 2018). Nonetheless, convective mixing remains a persistent aspect of the dissolution process since it arises due to the interaction between water and CO_2 coming from above, causing a denser layer of CO_2-saturated water to form atop a less dense water layer, as previously discussed (Erfani, 2020). It is worth mentioning that other existing methods are based on the utilization of nuclear magnetic resonance (NMR) (Liger-Belair et al., 2003), computer-assisted tomography (Eide et al., 2016; Trevisan et al., 2013), and microfluidic devices (Khalifi, 2021).

Measurements of the CO_2 diffusion coefficient in brine and pure water have been reported in the literature. Ratcliff and Holdcroft (1963) provided data on the diffusion coefficient of CO_2 at 25 °C and ~1 bar in sodium chloride (NaCl) concentrations ranging between (0–4) molar. They reported diffusion coefficient values within a range of (1.30–1.92) $\times 10^{-9}$ m^2/s, later compared and validated using molecular dynamics simulation (Huang, 2012). Correlation-based data on the diffusion coefficient of CO_2 in both pure water and seawater at varying salinities (0.6 and 1.2 molar) were presented by Al-Rawajfeh (2004), indicating a range of (1.74, 1.62, and 1.48) $\times 10^{-9}$ m^2/s. Lu et al. (2013) utilized a high-pressure capillary optical cell, placed horizontally to avoid convection. They used quantitative Raman spectroscopy to measure dissolved carbon dioxide concentration in time and distance. Their experiments were carried out over the range of −5 to 200 °C and 100 to 450 bar, with diffusion coefficient values ranging from 0.76×10^{-9} to 16.1×10^{-9} m^2/s. They concluded that while higher temperatures lead to higher diffusion coefficients, higher pressures lead to slightly lower diffusion coefficients for temperatures lower than 120 °C. Sell et al. (2013) measured the diffusion coefficient of CO_2 in fluorescently tagged water/brine solutions in microfluidic devices, and an analytical model was fitted to CO_2 concentration data obtained from fluorescence intensity profiles. At a fixed temperature of 26 °C, reported diffusion coefficient values were 1.86×10^{-9} m^2/s for the pressure range of 5–50 bar, and 0.6×10^{-9} to 1.8×10^{-9} m^2/s for brine salinity range of 5 to 0 M, respectively at 5 bar. They observed that increasing salinity slows down the diffusion rate by up to three times, whereas pressure had no significant effects. Cadogan et al. (2014) utilized Taylor dispersion analysis to estimate the diffusion coefficient of CO_2 in pure water. They reported diffusion coefficient values in the range of (2.2–12.2) $\times 10^{-9}$ m^2/s at temperature and pressure ranges of (25–150) °C and (140–500) bar. Pressure variation was found to have a negligible effect on the diffusion coefficient values estimation. Cadogan et al. (2015) measured the tracer diffusion coefficient of magnetically labeled CO_2 utilizing pulse-field gradient NMR techniques, initially introduced by Liger-Belair et al. (2003). Diffusion coefficient values of CO_2 in a variety of water and brine solutions were estimated at a fixed temperature of 25 °C. Brine solutions were prepared with different salts at different molalities: NaCl
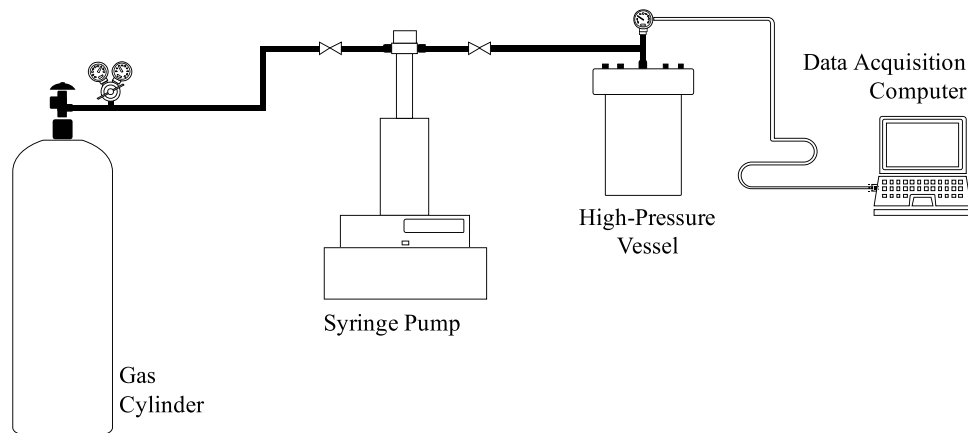
Fig. 1. Schematic diagram of the experimental setup: a gas cylinder, pump, pressure vessel, and data acquisition system that records the pressure and temperature of the vessel.
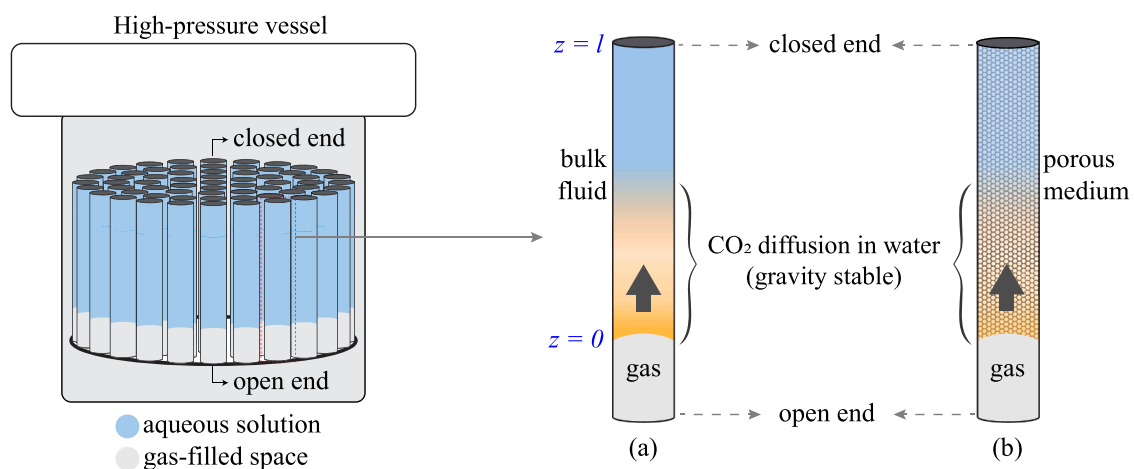

Fig. 2. Capillary tubes inside the high-pressure vessel, with their open ends facing down, filled with (a) bulk water/brine; and (b) water-saturated columns packed with glass beads.

(1–5) molal, $CaCl_2$ (0.9–2) molal, Na_2SO_4 (1) molal, and mixed salts (1.9) molal. Reported diffusion coefficient values ranged within $(1.25–2.13) \times 10^{-9}$ m²/s. Additionally, they pointed out that increasing salinity concentrations reduces diffusion coefficient values.

This work introduces a novel pressure-decay-based experimental approach to avoid density-driven convection mixing. Capillary tubes, with only one open end, were placed inside the reactor, with the open end facing downward, allowing the CO_2 to be transported from the lower to the upper (closed) side of the capillary tubes. A mathematical model Yang et al. (2019) was utilized to estimate the diffusion coefficient values. Several experiments were performed for up to 500 h, considering the effects of pressure and salinity. Estimated molecular diffusion coefficient values were found to be in accordance with the ones reported in the literature. Furthermore, the presented approach enables the measurement of effective molecular diffusion in porous media systems. We illustrate this capability by studying glass bead systems and measuring the impact of grain size on the effective molecular diffusion of CO_2 in water.

2. Materials and methods

2.1. Pressure-Decay-Based experimental setup

Riazi (1996) introduced the pressure-decay method, in which the diffusion coefficient of the gas in hydrocarbon systems was measured.

The experimental workflow of this technique consists of introducing a known amount of gas phase into a fixed-volume vessel containing the liquid phase. With time, part of the gas phase gets dissolved and diffuses into the liquid phase, causing the system pressure to drop. The temperature of the experimental setup is kept constant during the mass transfer process, and the pressure is continuously recorded. The diffusion coefficient is obtained from data-fitting the pressure data to an appropriate mathematical model. This technique was extensively used for gas-hydrocarbon systems (Saboorian-Jooybari, 2012; Sheikha et al., 2006; Zhang et al., 2000) since convective mixing can be conveniently neglected. However, despite its advantageous simplicity for laboratory applications, it is not suitable for determining the diffusion coefficient of CO_2 in water/brine systems because convective mixing cannot be neglected due to density-driven instabilities (Erfani, 2020). To isolate the natural convection phenomena during CO_2 dissolution, we modified the experimental work of Riazi (1996). The schematic of the experimental setup is presented in Fig. 1. Capillary tubes were then placed within a high-pressure vessel (Series 4540, 600 mL, Parr Instrument Company, USA) with their open ends facing down (see Fig. 2). Capillary forces were responsible for retaining water within the capillary tubes. A total of 62 in-house manufactured borosilicate capillary tubes (all with a diameter of 4.2 mm and length of 10 cm) were utilized for two sets of experiments. In the first set of experiments, capillary tubes were filled with the bulk aqueous phase up to a height of 8 cm. In the second set of experiments capillary tubes were filled with water-saturated columns

Table 2
Experimental conditions and estimated values of diffusion coefficient.

#	Initial Pressure (bar)	Grain Size μm	[NaCl] (mol/l)	Duration (hours)	Diffusion Coefficient ($\times 10^{-9}$ m^2/s)	λ	H bar/[kg/m^3]
1	15	Bulk fluid	0	300	2.91	3.81	0.65
2	15		1	300	2.46	6.34	1.07
3	15		5	300	1.28	7.62	1.28
4	30		0	300	2.83	3.91	0.62
5	50		0	300	2.82	8.00	0.98
6	15	[45–90]	0	500	1.64	6.54	0.48
7	15	[200–300]	0	500	1.80	6.77	0.50
8	15	[425–560]	0	500	1.97	7.57	0.55
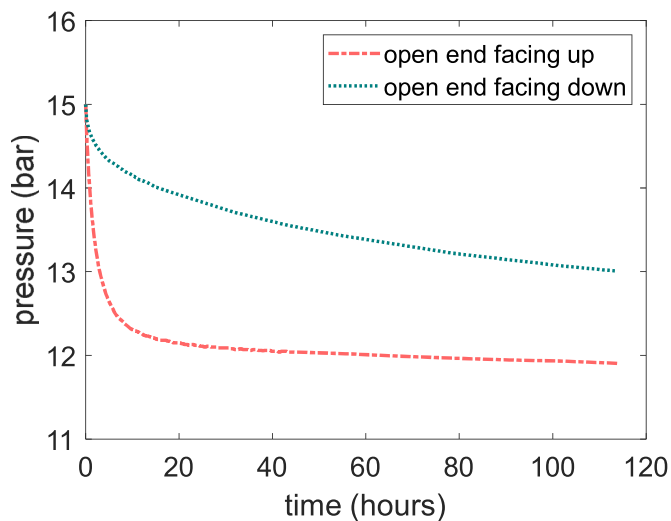
Fig. 3. Pressure drop versus time under two different arrangements of capillary tubes.

packed with glass beads with three different grain size ranges [45–90 μm], [200–300 μm], and [425–560 μm], up to a height of 8 cm. Then, we injected 100 ml of CO_2 gas into the vessel. Once the gas phase was introduced, the gas started dissolving into the liquid. Placing the capillary tubes with their open end facing down allowed the CO_2 mass transport to occur from the lower (open) end to the upper (closed) end of the capillary tubes (see Fig. 2). With a total volume of 93 ml of water, we could obtain a clear pressure decay profile.

Deionized water used in this study was obtained from a direct water purification system (Milli-Q, 8 l/h, Sigma Aldrich, USA) using a 0.22 μm membrane filter (Millipak Express 40, Sigma Aldrich). Carbon dioxide (99.995 % pure) was purchased from Air Liquide (Alphagaz line), and sodium chloride (NaCl) was purchased from Fisher Chemical.

We used a high-pressure syringe pump (100DX, Teledyne ISCO Inc., USA) with a working pressure of up to 685 bar. The high-pressure vessel had a maximum working pressure and temperature of 345 bar and 350 °C, respectively, which was also equipped with release valves, type J thermocouple, a pressure transducer, and a pressure gauge. We also used an expanded reactor controller (Series 4848B, Parr Instrument Company, USA) with available connections for pressure and temperature inputs. It is also equipped with a packaged temperature control unit (±2 °C system accuracy) within an operating temperature range of 0–800 °C.

2.2. Experimental workflow

The experimental workflow for each test consisted of the steps outlined below:

1. Deionized water, saline solutions, and glass beads were vacuumed for at least 72 h prior to starting each test to remove any dissolved or trapped air. Saline solutions were prepared by dissolving a calculated amount of NaCl into deionized water.
2. Carbon dioxide was transferred from the gas cylinder to the syringe pump and allowed to stand for at least 2 h before introducing it to the high-pressure vessel to avoid drastic temperature changes.
3. Capillary tubes were gently filled with the aqueous phase up to a height of 8 cm. In the case of columns with glass beads, we poured small amounts of glass beads and water and placed the tube on a shaker to ensure tight packing and cause any trapped air bubbles to escape. Then, more glass beads and water were added, and the procedure was repeated until the desired height of the porous medium was reached. Thereafter, capillary tubes were gently placed into the high-pressure vessel.
4. High-pressure vessel was carefully closed, tightened, and vacuumed to remove the air as much as possible.
5. Carbon dioxide was transferred by the syringe pump to the high-pressure vessel. Subsequently, the inlet and syringe pump valves were closed, and the CO_2 source disconnected to prevent any additional gas from entering the system.
6. As the CO_2 dissolved into the aqueous phase, pressure and temperature were continuously monitored and recorded for up to 500 h.

2.3. Determination of diffusion coefficients

Recorded pressure decay is utilized to determine the mass transfer of CO_2 into the aqueous phase through dissolution and molecular diffusion. General assumptions were made to describe the mass transfer process within each capillary tube. We assume that temperature was constant during each test since the effect of temperature variations of less than ± 0.5 °C can be neglected. Water evaporation is disregarded, given the negligible contribution of water vapor to the experimental pressure drop (Greenwood and Earnshaw, 1997). Swelling effects are considered negligible during the diffusion process, as they were observed to be less than 2 % in CO_2-water/brine systems (Khalifi et al., 2020; Khan et al., 2023). We assumed a constant diffusion of dissolved CO_2 since CO_2 remains low in each capillary tube under given experimental conditions. A constant compressibility factor was assumed during the pressure decay test, as less than 5 % variation in the compressibility factor is expected (Azin et al., 2013). In addition, our experimental approach allows the disregard of density-induced convection during the diffusion process, and therefore dispersion is irrelevant. Thus, assuming one-dimensional constant diffusion of dissolved CO_2 within each capillary tube, it can be described by Fick's second law (Fick, 1855):

$$\frac{\partial c}{\partial t} = D \frac{\partial^2 c}{\partial z^2} \tag{1}$$

where c is the concentration of gas molecules in the aqueous phase [ML^{-3}]; t is time, [T]; z is the distance from the interface, [L]; D is the diffusion coefficient of gas molecules, [L^{2}T^{-1}].

Eq. (1) should be solved subject to initial and boundary conditions. At the beginning of the pressure decay test, the water/brine contained in
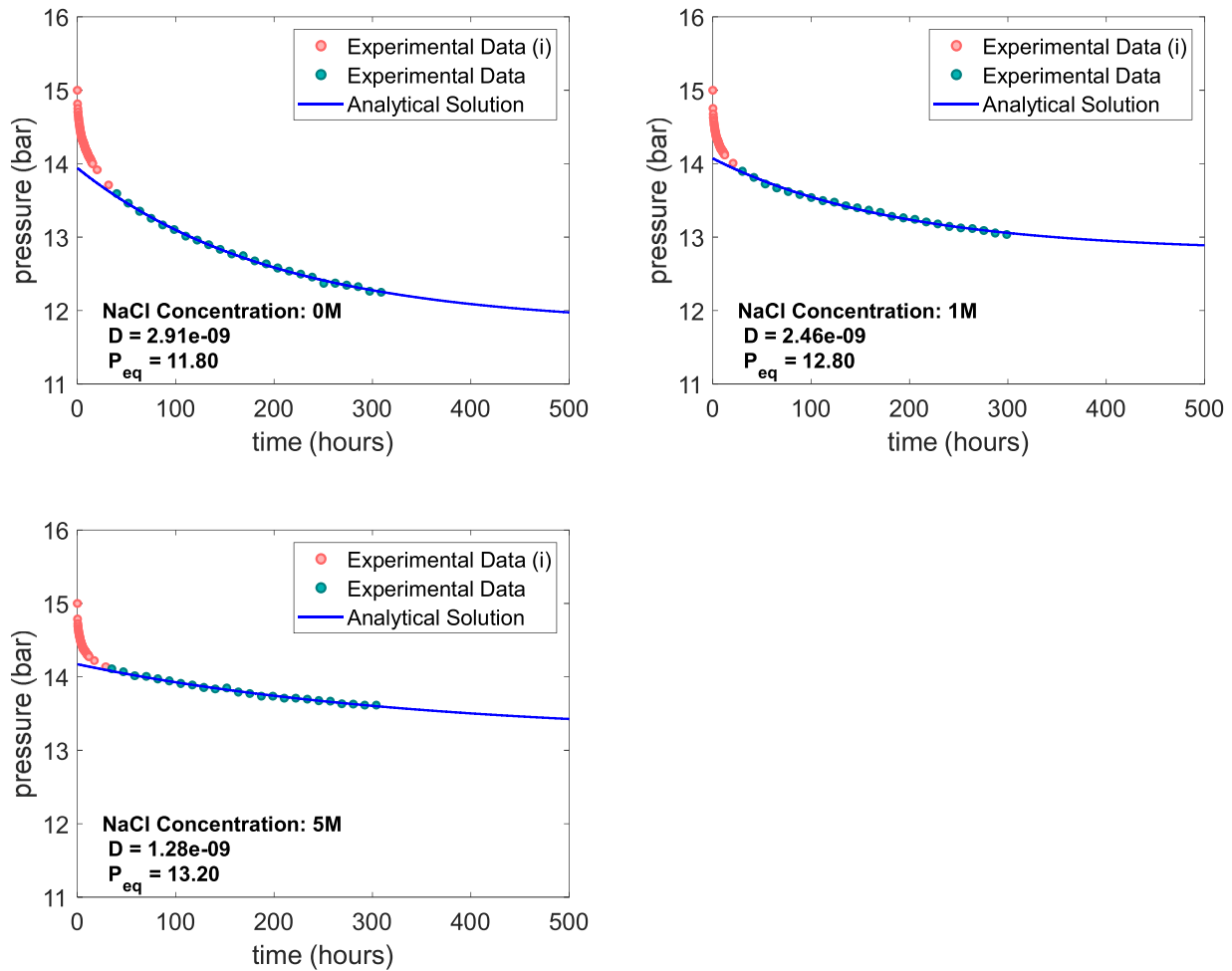
Fig. 4. Effect of salinity on value of diffusion coefficient.

the capillary tubes does not contain any CO_2. Hence, the initial condition is defined as:

$$c(z,t)|_{t=0} = 0, \quad \forall\, z \in [0,l] \tag{2}$$

The concentration of CO_2 in the water at the gas/liquid interface, where the equilibrium between the two phases is established, is considered the maximum available at the existing gas pressure:

$$c(z,t)|_{z=0} = c_s[p(t)] \quad \forall\, t > 0 \tag{3}$$

The capillary tubes exhibit significant length in comparison to the slow nature of the molecular diffusion process. It is reasonable to assume that the concentration of CO_2 is negligible at the closed end of the capillary tube, and that the experimental time is not enough to allow the closed-end capillary tube to affect the rate of mass transfer between the CO_2 and the water. This is a valid assumption adopted and demonstrated by previous researchers (Sheikha et al., 2006; Zarghami et al., 2017):

$$\left.\frac{\partial c(z,t)}{\partial z}\right|_{z=l} = 0 \tag{4}$$

where l is the height of the aqueous phase column, [L]; c_s is the CO_2 concentration in the liquid at the gas/liquid interface, [ML^{-3}]. Various models have been suggested for relating c_s to gas pressure p_g (Riazi et al., 1994; Riazi and Whitson, 1993b). One simple assumption is to assume the gas/liquid interface to have the maximum solubility of CO_2 at the prevailing gas pressure (Tharanivasan et al., 2004), which is assumed to be prescribed by Henry's law:

$$c_s = p_g / MH \tag{5}$$

where M is the molecular mass of gas, [MN^{-1}]; and H is Henry's constant for CO_2 gas, [L^{2}T^{-2}]. The temporal change of gas pressure in the cell, p_g [ML^{-1}T^{-2}], is related to the rate of dissolution of gas into water (at the gas-water interface), which in turn is equal to the diffusion mass flux at $z = 0$:

$$\frac{V_g}{ZR_gT}\frac{dp_g(t)}{dt} = DA\left.\frac{\partial c(z,t)}{\partial z}\right|_{z=0} \tag{6}$$

where A is the total area of the gas-water interface, [L^2], V_g is the gas volume, [L^3], Z is the gas compressibility factor, R_g is the gas constant, [ML^{2}T^{-2}K^{-1}], T is the absolute temperature, [t]. This equation is subject to the initial condition $p_g(t)|_{t=0} = p_i$.

The exact analytical solution of Eqs. (1)–(6) was presented by Yang et al. (2019), resulting in:

$$p_g = p_{eq} + p_i \sum_{n=1}^{\infty} \frac{2\lambda}{1 + \lambda + \lambda^2 a_n^2} e^{-\frac{Da_n^2 t}{l^2}} \tag{7}$$

where p_{eq} is the final (equilibrium) gas pressure, and a_n is the nth non-zero positive root of:

$$\tan(a_n) = -\lambda a_n \tag{8}$$
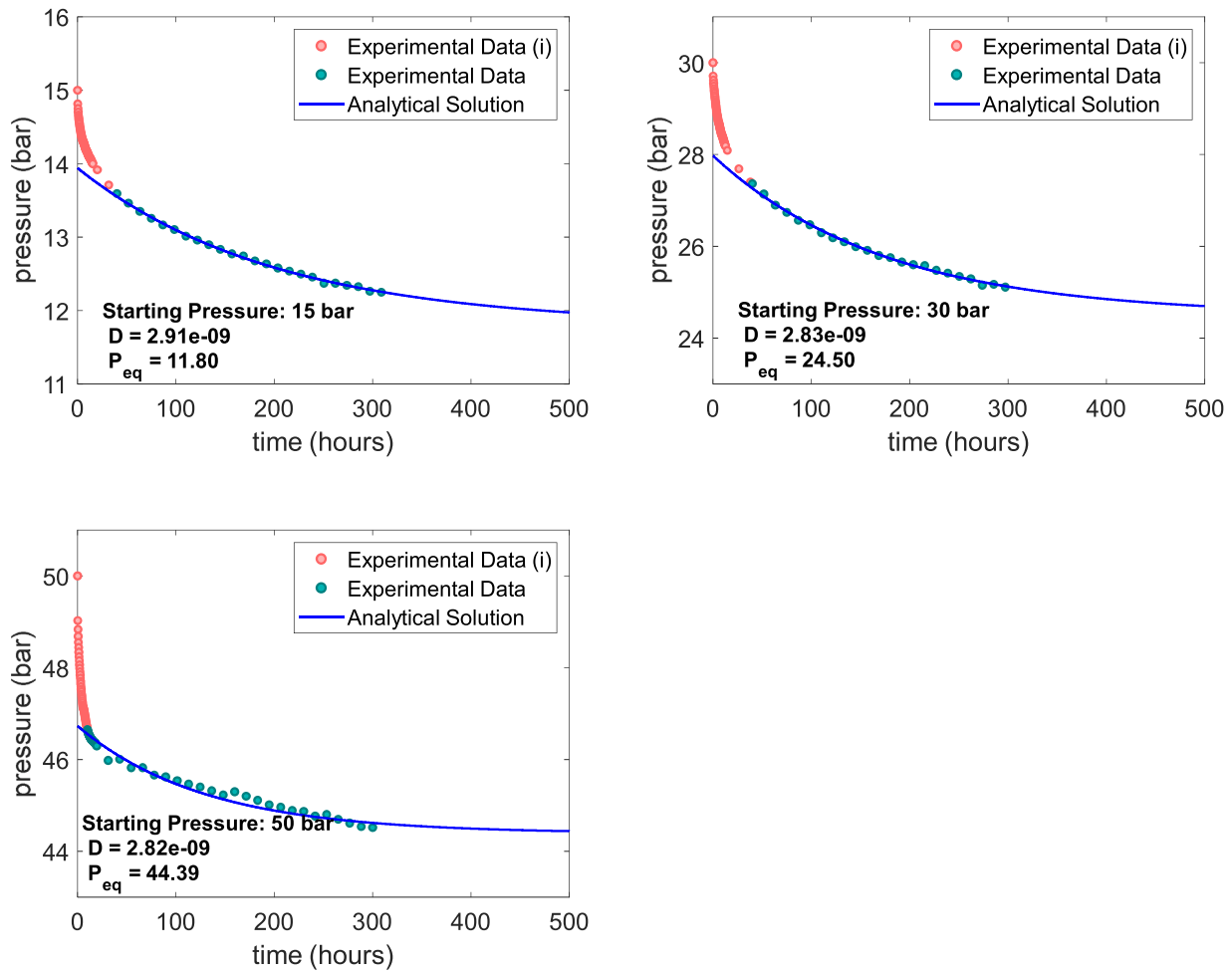
where λ is defined by:

Fig. 5. Effect of pressure on determined diffusion coefficients.

$$\lambda = \frac{p_{eq}}{p_i - p_{eq}} \qquad (9)$$

Also, by combining the real gas law with mass conservation, and assuming that the gas concentration in the liquid at equilibrium is constant everywhere, we can show:

$$(p_i - p_{eq})V_g = Z c_{eq} V_{liquid} R_g T$$

$$\lambda = \frac{p_{eq}}{p_i - p_{eq}} = \frac{V_g M H}{V_{liquid} Z R_g T} \qquad (10)$$

where V_{liquid} is the aqueous phase volume, [L^3].

By fitting the infinite-series solution, presented in Eq. (7), to the measured pressure decay data, we can estimate the corresponding values of λ and D. Knowing λ, we can calculate the equilibrium gas pressure p_{eq} from Eq. (9), Henry's constant from Eq. (10), and CO_2 solubility in water at a given equilibrium pressure from Eq. (5). The present study considers a range of defined equilibrium pressures as a starting point for estimating the values of λ, from which D is calculated. When calculated, these values correspond to the minimum squared norm-2 of the residual. It is noteworthy that the squared 2-norm has been computed for all experiments, affirming the minimal deviation of the analytical solution from the experimental data. Appendix A describes the approximation process of the estimated diffusion coefficients. Some of these results are reported in Table 2. In this analysis, we present our results based only on the first term of the infinite-series solution, presented in Eq. (11). In Appendix B, we investigate the sensitivity of including more terms and show that the effect of using higher-order terms is insignificant.

$$\frac{p_g - p_{eq}}{p_i} = \frac{2\lambda}{1 + \lambda + \lambda^2 a_1^2} e^{-\frac{D a_1^2 t}{l^2}} \qquad (11)$$

Where a_1 is the first positive non-zero root of Eq. (8). This approximate equation is not valid for early times but gives a good representation of the late-time solution. The equation presented above requires the equilibrium pressure to determine the diffusion coefficient. Theoretically, the equilibrium pressure is achieved once the aqueous phase is completely saturated with carbon dioxide. However, molecular diffusion is a very slow process that may take months to reach equilibrium, even at the laboratory scale (Tharanivasan et al., 2006).

3. Results and discussion

Eight sets of pressure-decay experiments were conducted at a constant temperature of 20 °C for more than 300 h (see Table 2). We studied the impact of salinity, pressure, and grain size on the diffusion coefficient. To test our experimental approach, we initially compared two different arrangements: (1) open-end facing up and (2) open-end facing down. As depicted in Fig. 3, the face-up configuration exhibits a much faster pressure drop than the face-down configuration. As explained in the Introduction, this is because in the faceup case, the CO_2 mass transfer occurs downward, resulting in an enhanced dissolution process driven by not only molecular diffusion but also natural convection (Erfani, 2020). This effect is clearly avoided when the open end is facing down.
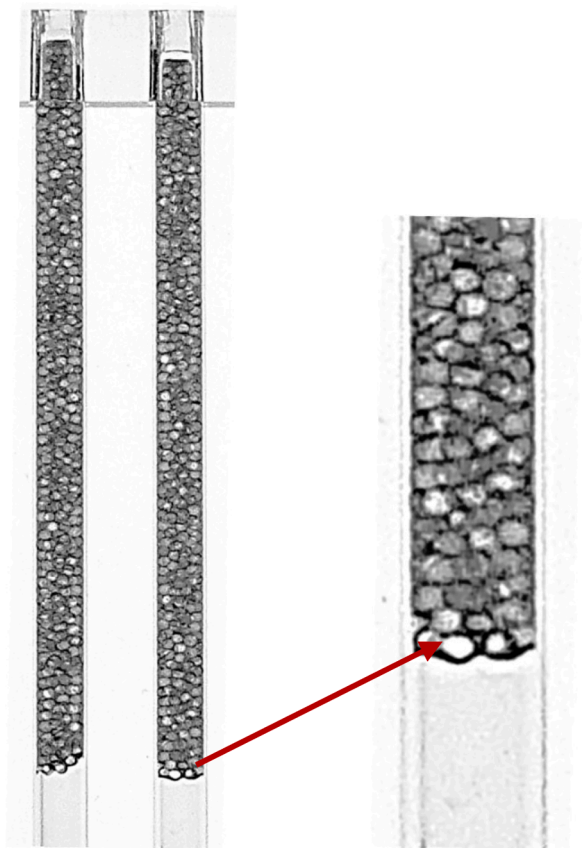
Fig. 6. Capillary tubes, with the open end facing downwards, filled with glass beads and deionized water. Image was conveniently gray-scaled for visualization purposes.

3.1. Effect of salinity and gas pressure on CO_2 diffusion coefficient in bulk water

As shown in Table 2, four experiments, with NaCl concentration ranging from 0.0 to 5.0 M were performed. Experimental data, along with the fitted curve, are shown in Fig. 4. As we used Eq. (11) for fitting the data, we excluded the early-time data (those shown as red dots), from the fitting procedure and fitted the remaining data (shown as blue dots). The fitted curve is represented by a solid blue line. Estimated diffusion coefficient values range from 2.91×10^{-9} m²/s to 1.28×10^{-9} m²/s, decreasing as salinity concentration increases. This is in line with results found in previous studies (Belgodere et al., 2015).

The effect of gas pressure was taken into account by performing experiments at three different pressures: 15, 30, and 50 bar as presented in Fig. 5. Estimated diffusion coefficients range between 2.82×10^{-9} m²/s and 2.91×10^{-9} m²/s. Clearly, the gas pressure did not have a major impact on the value of the diffusion coefficient. This is consistent with expectations and previous studies (Sell et al., 2013).

Although the current investigation was carried out at a temperature of 20 °C, the methodology employed can be extended to higher temperatures of up to 80 °C. It should be noted that beyond 80 °C, the capillary tubes are unable to retain the aqueous phase.

3.2. Impact of grain size on the effective molecular diffusion in a porous medium

Molecular diffusion of a solute in a liquid is known to be slower in a porous medium than in a bulk liquid (Gao et al., 2019). This is mainly due to: (1) a smaller cross-sectional area available for the diffusive mass transport, and (2) a longer transport distance because of the porous

medium tortuosity, defined as the ratio of the actual flow path to the straight distance between the ends of the flow path (Bear, 2013). Fick's second law can still be applied to describe the CO_2 molecular diffusion in porous media (Rezk et al., 2022). Fig. 6 depicts capillary tubes filled with water-saturated glass beads to represent the porous medium. Fig. 7 shows the data and the fitted curves for the three experiments.

In order to account for the aforementioned effects, the previous diffusion coefficient D should be corrected for the tortuosity τ (dimensionless), resulting in a smaller effective diffusion coefficient, D_e as follows (Petersen, 1958; Ullman and Aller, 1982; van Brakel and Heertjes, 1974):

$$D_e = \frac{D}{\tau^2} \tag{12}$$

The values of $\tau^2 \geq 1$ imply that the species, during diffusion in the interstitial fluid of a porous medium, follow a longer average path than in the absence of the solid (Boudreau, 1996). Estimated effective diffusion coefficient values resulted in 1.64×10^{-9} m²/s for grain sizes raging [45–90] μm, 1.80×10^{-9} m²/s for grain size raging [200–300] μm, and 1.97×10^{-9} m²/s for grain size raging [425–560] μm. The values of τ^2, in the order of precedence, are 1.77, 1.62, and 1.48, which shows that higher tortuosity values lead to lower effective diffusion coefficient values (Barrande et al., 2007; Lanfrey et al., 2010).

Furthermore, we conducted a validation experiment to measure the solubility of CO_2 in water at 20 °C. We used the pressure decay experimental approach, which is illustrated in Fig. 1. We added deionized water into a high-pressure vessel and then vacuumed the vessel to evacuate any air presence. As we stirred the water at 400 rpm, carbon dioxide was then transferred into the high-pressure vessel. We stopped the experiment once the pressure stabilized. We recorded the initial and final pressure readings to calculate the solubility of CO_2 in water by using Eq. (10). The calculated solubility value was 0.419 mol/kgH₂O. The literature reports a value of 0.431 mol/kgH₂O for the solubility of CO_2 in water (Lucile et al., 2012) at 25 °C and values. Also, the solubility value of 0.432 mol/kgH₂O at 20 °C, is obtained using commercial simulators. The experimental approach proposed in this study yielded a calculated CO_2 solubility in water of 0.428 mol/kgH₂O, which is consistent with the solubility values mentioned earlier.

4. Conclusions

Our proposed experimental approach enables the determination of CO_2 diffusion coefficient values in water, under a variety of conditions, by utilizing the conventional pressure decay method. This work examines the dissolution and diffusion process of carbon dioxide in pure water and brine solutions, utilizing traditional pressure decay experiments to determine the molecular diffusion coefficient at different salt concentrations, pressures, and porous media, at a temperature of 20 °C. We found that diffusion coefficient values (1) decreased with increasing the salinity of the aqueous phase, (2) were not significantly affected by pressure changes, and (3) increased with increasing the grain diameter of the porous media. We present a new straightforward yet accurate experimental workflow to determine diffusion coefficient values of CO_2 in brine/water. In particular, we successfully eliminate density-driven instabilities that result in natural convection, which would otherwise lead to unrealistically large values of diffusion coefficient. Our experimental results are in agreement with earlier studies. This method allows us to determine not only the diffusion coefficient but also Henry's coefficient. Furthermore, this experimental approach enables the potential to perform specific reservoir-targeted tests, focusing on the relation of diffusion processes with porous media characteristics, which is the focus of our upcoming research.

CRediT authorship contribution statement

Enoc Basilio: Investigation, Methodology, Software, Visualization,
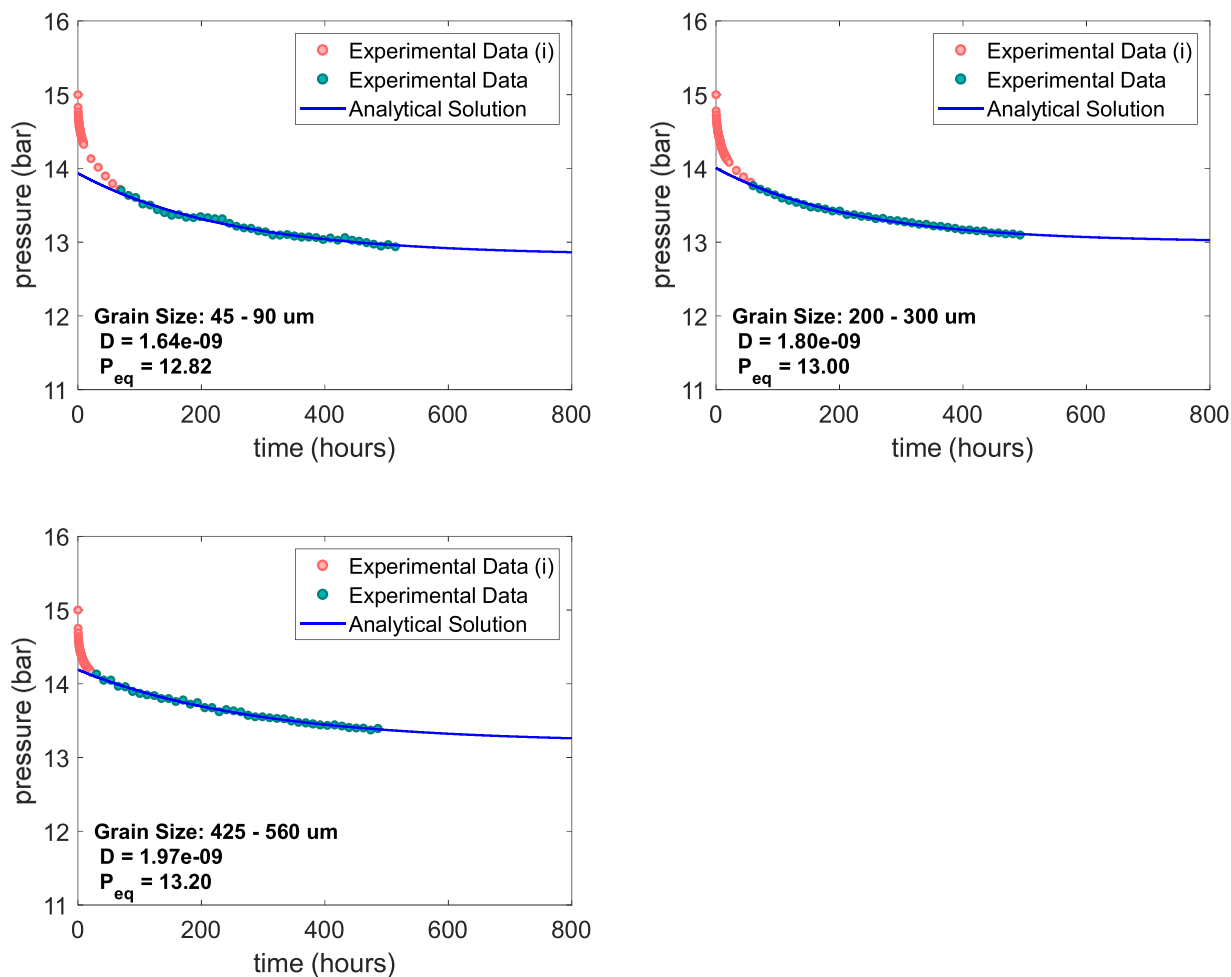
Fig. 7. Effect of porous media grain size on diffusion coefficients.

Writing – original draft. **Mouadh Addassi:** Investigation, Methodology, Software, Writing – review & editing. **Mohammed Al-Juaied:** Validation, Writing – review & editing. **S. Majid Hassanizadeh:** Methodology, Validation, Writing – review & editing. **Hussein Hoteit:** Conceptualization, Funding acquisition, Methodology, Supervision, Validation, Writing – review & editing.

Declaration of Competing Interest

The authors declare that they have no known competing financial interests or personal relationships that could have appeared to influence the work reported in this paper.

Data availability

The link for the data and code are shared in the manuscript.

Appendix A: Calculation of diffusion coefficients

Mass transfer experiments frequently demand an extensive duration to achieve equilibrium pressure. We conducted our tests for a sufficiently prolonged period to approach the final equilibrium pressure closely, allowing for sensitivity analysis around this final pressure. In our investigation, we computed diffusion coefficients in the vicinity of the obtained final pressure, considering that the equilibrium pressure is expected to be lower than the final pressure. These pressure values, considered individually as equilibrium pressure, were utilized as an initial value to estimate the values of λ, from which D is calculated. Among the obtained diffusion coefficient values, the one corresponding to the minimum squared 2-norm of the residual between the experimental data and the values computed from the infinite-series solution was deemed the optimized value, as presented in Fig. A1.
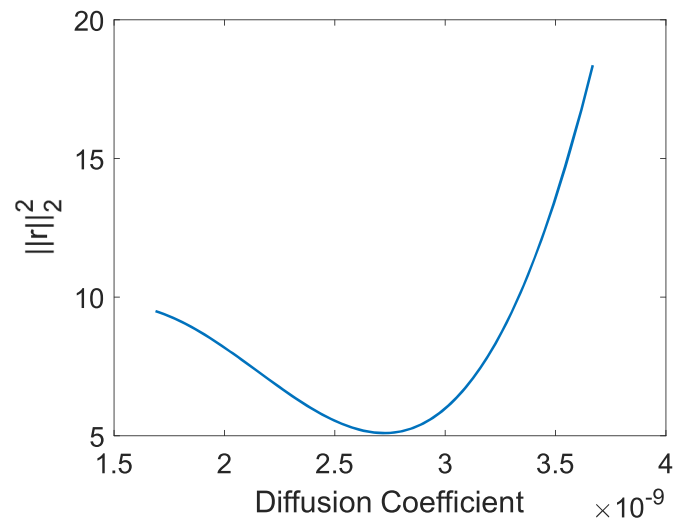
Fig. A1. Estimation of the diffusion coefficients by minimizing the squared 2-norm of the residual between the experimental data and the values computed from the infinite-series solution.

Appendix B: Sensitivity of the infinite-series solution

The solution in Eq. (7) includes an infinity series which depends on the infinite solutions, λ, of $\tan(a_n) + \lambda a_n = 0$. We calculated the solutions, λ, with the bisection method, which was found to be more robust than other higher-order methods (such as the Newton-Raphson method), especially when n increases beyond 10, where the nonlinearity of the system increases.

To investigate the sensitivity of the infinite series on the solution, we calculated the pressure solution by considering different numbers of terms in the series. To compare the performance of using different numbers of terms of the infinite-series solution, we considered our base-case experimental dataset, pressure-decay in deionized water. We then fit the data using the first, second, and twenty-fifth terms of the series. Fig. B1 shows the experimental data with the matching solutions. The turquoise dots correspond to the experimental data, and the curves correspond to the fitted series solutions. The blue curve corresponds to the solution with the first term only of the series, the magenta curve corresponds to using the first two terms of the series, and the black curve corresponds to using 25 terms. We find that the first term of the series provides a reasonable fit for the late-time solution. However, using more terms of the series results in a better representation of the early times. Estimated diffusion coefficient values are not significantly impacted if more than one term is used. All data and source code are provided in (Hoteit, 2023).
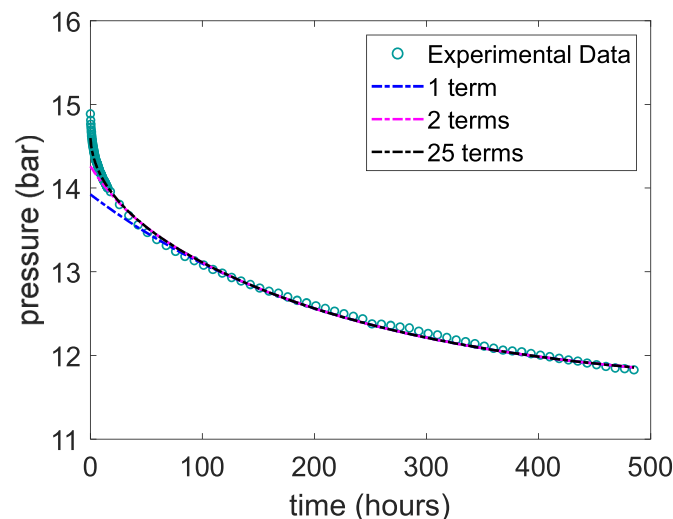

Fig. B1. Matching experimental pressure-decay data using 1, 2, and 25 terms of the infinite-series solution, showing that the higher-order terms only impact the early time of the pressure decay, but they don't affect the overall match of the data at later times.

References

Adams, J.J., Bachu, S., 2002. Equations of state for basin geofluids: algorithm review and intercomparison for brines. Geofluids 2, 257–271. https://doi.org/10.1046/j.1468-8123.2002.00041.x.

Addassi, M., Omar, A., Hoteit, H., Afifi, A.M., Arkadakskiy, S., Ahmed, Z.T., Kunnummal, N., Gislason, S.R., Oelkers, E.H., 2022. Assessing the potential of solubility trapping in unconfined aquifers for subsurface carbon storage. Sci. Rep. 12, 20452. https://doi.org/10.1038/s41598-022-24623-6.

Ahmadi, H., Jamialahmadi, M., Soulgani, B.S., Dinarvand, N., Sharafi, M.S., 2020. Experimental study and modelling on diffusion coefficient of CO2 in water. Fluid Phase Equilib. 523, 112584 https://doi.org/10.1016/j.fluid.2020.112584.

Alqahtani, A., He, X., Yan, B., Hoteit, H., 2023. Uncertainty analysis of CO2 storage in deep saline aquifers using machine learning and bayesian optimization. Energies 16, 1684. https://doi.org/10.3390/en16041684.

Al-Rawajfeh, A.E., 2004. Modelling and Simulation of CO2 Release in Multiple-Effect Distillers For Seawater Desalination (Doctoral Thesis). Universitäts- und Landesbibliothek Sachsen-Anhalt. https://doi.org/10.25673/3764.

Azin, R., Mahmoudy, M., Raad, S., Osfouri, S., 2013. Measurement and modeling of CO2 diffusion coefficient in Saline Aquifer at reservoir conditions. Open Eng. 3, 585–594. https://doi.org/10.2478/s13531-012-0069-2.

Bachu, S., Adams, J.J., 2003. Sequestration of CO2 in geological media in response to climate change: capacity of deep saline aquifers to sequester CO2 in solution. Energy Convers. Manage. 44, 3151–3175. https://doi.org/10.1016/S0196-8904(03)00101-8.

Barrande, M., Bouchet, R., Denoyel, R., 2007. Tortuosity of porous particles. Anal. Chem. 79, 9115–9121. https://doi.org/10.1021/ac071377r.

Bear, J., 2013. Dynamics of fluids in porous media. Courier Corporation.

Belgodere, C., Dubessy, J., Vautrin, D., Caumon, M.C., Sterpenich, J., Pironon, J., Robert, P., Randi, A., Birat, J.P., 2015. Experimental determination of CO2 diffusion coefficient in aqueous solutions under pressure at room temperature via Raman spectroscopy: impact of salinity (NaCl). J. Raman Spectrosc. 46, 1025–1032. https://doi.org/10.1002/jrs.4742.

Boudreau, B.P., 1996. The diffusive tortuosity of fine-grained unlithified sediments. Geochim. Cosmochim. Acta 60, 3139–3142. https://doi.org/10.1016/0016-7037(96)00158-5.

Cadogan, S.P., Hallett, J.P., Maitland, G.C., Trusler, J.P.M., 2015. Diffusion coefficients of carbon dioxide in brines measured using 13C pulsed-field gradient nuclear magnetic resonance. J. Chem. Eng. Data 60, 181–184. https://doi.org/10.1021/je5009203.

Cadogan, S.P., Maitland, G.C., Trusler, J.P.M., 2014. Diffusion coefficients of CO2 and N2 in water at temperatures between 298.15 K and 423.15 K at pressures up to 45 MPa. J. Chem. Eng. Data 59, 519–525. https://doi.org/10.1021/je401008s.

Davison, J., Freund, P., Smith, A., 2001. Putting Carbon Back Into the Ground. IEA Greenhouse Gas R&D Programme, Cheltenham.

Eide, Ø., Fernø, M.A., Alcorn, Z., Graue, A., 2016. Visualization of carbon dioxide enhanced oil recovery by diffusion in fractured chalk. SPE J. 21, 112–120. https://doi.org/10.2118/170920-PA.

Emami-Meybodi, H., Hassanzadeh, H., Green, C.P., Ennis-King, J., 2015. Convective dissolution of CO2 in saline aquifers: progress in modeling and experiments. Int. J. Greenh. Gas Control 40, 238–266. https://doi.org/10.1016/j.ijggc.2015.04.003. Special Issue commemorating the 10th year anniversary of the publication of the Intergovernmental Panel on Climate Change Special Report on CO2 Capture and Storage.

Erfani, H., 2020a. Comments on the paper "experimental study and modelling on diffusion coefficient of CO2 in water" by H. Ahmadi et al. (2020). Fluid Phase Equilib. 524, 112791 https://doi.org/10.1016/j.fluid.2020.112791.

Erfani, H., Babaei, M., Niasar, V., 2020b. Signature of Geochemistry on density-driven CO mixing in sandstone aquifers. Water Resour. Res. 56 https://doi.org/10.1029/2019WR026060 e2019WR026060.

Fick, A., 1855. Ueber diffusion. Ann. Phys. 170, 59–86. https://doi.org/10.1002/andp.18551700105.

Firoozabadi, A., Myint, P.C., 2010. Prospects for subsurface CO2 sequestration. AlChE J. 56, 1398–1405. https://doi.org/10.1002/aic.12287.

Gao, H., Zhang, B., Fan, L., Zhang, H., Chen, G., Tontiwachwuthikul, P., Liang, Z., 2019. Study on diffusivity of CO2 in oil-saturated porous media under high pressure and temperature. Energy Fuels 33, 11364–11372. https://doi.org/10.1021/acs.energyfuels.9b01947.

Garcia, J.E., 2001. Density of Aqueous Solutions of CO2 (No. LBNL-49023). Lawrence Berkeley National Lab. (LBNL), Berkeley, CA (United States). https://doi.org/10.2172/790022.

Getling, A.V., 2012. Rayleigh-Bénard convection. Scholarpedia 7, 7702. https://doi.org/10.4249/scholarpedia.7702.

Ghasemi, M., Astutik, W., Alavian, S.A., Whitson, C.H., Sigalas, L., Olsen, D., Suicmez, V. S., 2016. Determining diffusion coefficients for carbon dioxide injection in oil-saturated chalk by use of a constant-volume-diffusion method. SPE J. 22, 505–520. https://doi.org/10.2118/179550-PA.

Ghorayeb, K., Firoozabadi, A., 2000. Modeling multicomponent diffusion and convection in porous media. SPE J. 5, 158–171. https://doi.org/10.2118/62168-PA.

Greenwood, N.N., Earnshaw, A., 1997. Chemistry of the Elements. Butterworth-Heinemann, Oxford. https://doi.org/10.1016/B978-0-7506-3365-9.50014-6.

Hoteit, H., 2013. Modeling diffusion and gas–oil mass transfer in fractured reservoirs. J. Pet. Sci. Eng. 105, 1–17. https://doi.org/10.1016/j.petrol.2013.03.007.

Hoteit, H., Firoozabadi, A., 2018. Modeling of multicomponent diffusions and natural convection in unfractured and fractured media by discontinuous Galerkin and mixed methods. Int. J. Numer. Methods Eng. 114, 535–556. https://doi.org/10.1002/nme.5753.

Hoteit, H., Firoozabadi, A., 2009. Numerical modeling of diffusion in fractured media for gas-injection and -recycling schemes. Spe J. 14, 323–337.

Huang, T., 2012. Molecular Dynamics Simulation of Carbon Dioxide in Aqueous Electrolyte Solution. Swinburne University of Technology.

Jafari Raad, S.M., Emami-Meybodi, H., Hassanzadeh, H., 2016. On the choice of analogue fluids in CO2 convective dissolution experiments. Water Resour. Res. 52, 4458–4468. https://doi.org/10.1002/2015WR018040.

Jafari Raad, S.M., Hassanzadeh, H., 2016. Does impure CO2 impede or accelerate the onset of convective mixing in geological storage? Int. J. Greenh. Gas Control 54, 250–257. https://doi.org/10.1016/j.ijggc.2016.09.011.

Kantzas, A., Bryan, J., Taheri, S., 2022. Molecular diffusion. Fundamentals of Fluid Flow in Porous Media.

Khalifi, M., 2021. Experimental Measurement of Diffusion Coefficient of Gaseous Solvents in Liquids (Doctoral Thesis). Schulich School of Engineering. https://doi.org/10.11575/PRISM/38865.

Khalifi, M., Sabet, N., Zirrahi, M., Hassanzadeh, H., Abedi, J., 2020. Concentration-dependent molecular diffusion coefficient of gaseous ethane in liquid toluene. AlChE J. 66, e16966. https://doi.org/10.1002/aic.16966.

Khan, M., Nath, D., Khalifi, M., Hassanzadeh, H., 2023. Measurements and modeling of the dissolution and exsolution kinetics of the ethane/n-heptane system. Ind. Eng. Chem. Res. 62, 775–788. https://doi.org/10.1021/acs.iecr.2c03454.

Koide, H., Tazaki, Y., Noguchi, Y., Nakayama, S., Iijima, M., Ito, K., Shindo, Y., 1992. Subterranean containment and long-term storage of carbon dioxide in unused aquifers and in depleted natural gas reservoirs. Energy Convers. Manage. 33, 619–626. https://doi.org/10.1016/0196-8904(92)90064-4.

Lackner, K.S., 2003. A Guide to CO2 sequestration. Science 300, 1677–1678. https://doi.org/10.1126/science.1079033.

Lanfrey, P.Y., Kuzeljevic, Z.V., Dudukovic, M.P., 2010. Tortuosity model for fixed beds randomly packed with identical particles. Chem. Eng. Sci. 65, 1891–1896. https://doi.org/10.1016/j.ces.2009.11.011.

Liger-Belair, G., Prost, E., Parmentier, M., Jeandet, P., Nuzillard, J.M., 2003. Diffusion coefficient of CO2 molecules as determined by 13C NMR in various carbonated beverages. J. Agric. Food Chem. 51, 7560–7563. https://doi.org/10.1021/jf034693p.

Lindeberg, E., Wessel-Berg, D., 1997. Vertical convection in an aquifer column under a gas cap of CO2. Energy conversion and management. In: Proceedings of the Third International Conference on Carbon Dioxide Removal 38, pp. S229–S234. https://doi.org/10.1016/S0196-8904(96)00274-9.

Lu, W., Guo, H., Chou, I.M., Burruss, R.C., Li, L., 2013. Determination of diffusion coefficients of carbon dioxide in water between 268 and 473K in a high-pressure capillary optical cell with in situ Raman spectroscopic measurements. Geochim. Cosmochim. Acta 115, 183–204. https://doi.org/10.1016/j.gca.2013.04.010.

Lucile, F., Cézac, P., Contamine, F., Serin, J.P., Houssin, D., Arpentinier, P., 2012. Solubility of carbon dioxide in water and aqueous solution containing sodium hydroxide at temperatures from (293.15 to 393.15) K and pressure up to 5 MPa: experimental measurements. J. Chem. Eng. Data 57, 784–789. https://doi.org/10.1021/je200991x.

MacMinn, C.W., Szulczewski, M.L., Juanes, R., 2011. CO2 migration in saline aquifers. Part 2. Capillary and solubility trapping. J. Fluid Mech. 688, 321–351. https://doi.org/10.1017/jfm.2011.379.

Macminn, C.W., Szulczewski, M.L., Juanes, R., 2010. CO2 migration in saline aquifers. Part 1. Capillary trapping under slope and groundwater flow. J. Fluid Mech. 662, 329–351. https://doi.org/10.1017/S0022112010003319.

Mehrotra, A.K., Garg, A., Svrcek, W.Y., 1987. Prediction of mass diffusivity of CO2 into bitumen. Can. J. Chem. Eng. 65, 826–832. https://doi.org/10.1002/cjce.5450650517.

Metz, B., Davidson, O., de Coninck, H., Loos, M., Meyer, L., 2005. Carbon Dioxide Capture and Storage. Intergovernmental Panel on Climate Change, New York.

Mohammadi, M., Khalifi, M., Sabet, N., Hassanzadeh, H., 2023. Experiments and reduced order modeling of symmetry breaking in Rayleigh-Taylor mixing. Phys. Rev. Fluids 8, 103504. https://doi.org/10.1103/PhysRevFluids.8.103504.

Nguyen, T.A., Ali, S.M.F., 1998. Effect of nitrogen on the solubility and diffusivity of carbon dioxide into oil and oil recovery by the immiscible WAG process. J. Can. Pet. Technol. 37 https://doi.org/10.2118/98-02-02.

Oelkers, E.H., Arkadakskiy, S., Afifi, A.M., Hoteit, H., Richards, M., Fedorik, J., Delaunay, A., Torres, J.E., Ahmed, Z.T., Kunnummal, N., Gislason, S.R., 2022. The subsurface carbonation potential of basaltic rocks from the Jizan region of Southwest Saudi Arabia. Int. J. Greenh. Gas Control 120, 103772. https://doi.org/10.1016/j.ijggc.2022.103772.

Omar, A., Addassi, M., Vahrenkamp, V., Hoteit, H., 2021. Co-optimization of co2 storage and enhanced gas recovery using carbonated water and supercritical co2. Energies 14, 7495. https://doi.org/10.3390/en14227495.

Petersen, E.E., 1958. Diffusion in a pore of varying cross section. AlChE J. 4, 343–345. https://doi.org/10.1002/aic.690040322.

Pruess, K., Zhang, K., 2008. Numerical Modeling Studies of The Dissolution-Diffusion-Convection ProcessDuring CO2 Storage in Saline Aquifers (No. LBNL-1243E). Lawrence Berkeley National Lab. (LBNL), Berkeley, CA (United States). https://doi.org/10.2172/944124.

Ratcliff, G., Holdcroft, J., 1963. Diffusivities of gases in aqueous electrolyte solutions. Trans. Inst. Chem. Eng. 41, 315–319.

Rezk, M.G., Foroozesh, J., Abdulrahman, A., Gholinezhad, J., 2022. CO2 diffusion and dispersion in porous media: review of advances in experimental measurements and mathematical models. Energy Fuels 36, 133–155. https://doi.org/10.1021/acs.energyfuels.1c03552.

Riazi, M.R., 1996. A new method for experimental measurement of diffusion coefficients in reservoir fluids. J. Pet. Sci. Eng. 14, 235–250. https://doi.org/10.1016/0920-4105(95)00035-6.

Riazi, M.R., Whitson, C.H., 1993a. Estimating diffusion coefficients of dense fluids. Ind. Eng. Chem. Res. 32, 3081–3088. https://doi.org/10.1021/ie00024a018.

Riazi, M.R., Whitson, C.H., 1993b. Estimating diffusion coefficients of dense fluids. Ind. Eng. Chem. Res. 32, 3081–3088. https://doi.org/10.1021/ie00024a018.

Riazi, M.R., Whitson, C.H., da Silva, F., 1994. Modelling of diffusional mass transfer in naturally fractured reservoirs. J. Pet. Sci. Eng. 10, 239–253. https://doi.org/10.1016/0920-4105(94)90084-1.

Saboorian-Jooybari, H., 2012. A novel methodology for simultaneous estimation of gas diffusivity and solubility in bitumens and heavy oils. In: Presented at the SPE Heavy Oil Conference Canada. OnePetro. https://doi.org/10.2118/157734-MS.

Sell, A., Fadaei, H., Kim, M., Sinton, D., 2013. Measurement of CO2 diffusivity for carbon sequestration: a microfluidic approach for reservoir-specific analysis. Environ. Sci. Technol. 47, 71–78. https://doi.org/10.1021/es303319q.

Sheikha, H., Mehrotra, A.K., Pooladi-Darvish, M., 2006. An inverse solution methodology for estimating the diffusion coefficient of gases in Athabasca bitumen from pressure-decay data. J. Pet. Sci. Eng. 53, 189–202. https://doi.org/10.1016/j.petrol.2006.06.003.

Sigmund, P.M., 1976. Prediction of molecular diffusion at reservoir conditions. Part 1-measurement and prediction of binary dense gas diffusion coefficients. J. Can. Pet. Technol. 15 https://doi.org/10.2118/76-02-05.

Spycher, N., Pruess, K., Ennis-King, J., 2003. CO2-H2O mixtures in the geological sequestration of CO2. I. Assessment and calculation of mutual solubilities from 12 to 100°C and up to 600bar. Geochim. Cosmochim. Acta 67, 3015–3031.

Tharanivasan, A.K., Yang, C., Gu, Y., 2006. Measurements of molecular diffusion coefficients of carbon dioxide, methane, and propane in heavy oil under reservoir conditions. Energy Fuels 20, 2509–2517. https://doi.org/10.1021/ef060080d.

Tharanivasan, A.K., Yang, C., Gu, Y., 2004. Comparison of three different interface mass transfer models used in the experimental measurement of solvent diffusivity in heavy oil. J. Pet. Sci. Eng. 44, 269–282. https://doi.org/10.1016/j.petrol.2004.03.003.

Trevisan, O.V., Araujo, S.V., Santos, R.G.D., Vargas, J.A., 2013. Diffusion coefficient of CO2 in light oil under reservoir conditions using X-Ray computed tomography. Presented at the OTC Brasil. OnePetro. https://doi.org/10.4043/24454-MS.

Ullman, W.J., Aller, R.C., 1982. Diffusion coefficients in nearshore marine sediments1. Limnol. Oceanogr. 27, 552–556. https://doi.org/10.4319/lo.1982.27.3.0552.

van Brakel, J., Heertjes, P.M., 1974. Analysis of diffusion in macroporous media in terms of a porosity, a tortuosity and a constrictivity factor. Int. J. Heat Mass Transf. 17, 1093–1103. https://doi.org/10.1016/0017-9310(74)90190-2.

Yang, X., Shao, Q., Hoteit, H., Carrera, J., Younes, A., Fahs, M., 2021. Three-dimensional natural convection, entropy generation and mixing in heterogeneous porous medium. Adv. Water Resour. 155, 103992 https://doi.org/10.1016/j.advwatres.2021.103992.

Yang, Z., Bryant, S., Dong, M., Hassanzadeh, H., 2019. An analytical method of estimating diffusion coefficients of gases in liquids from pressure decay tests. AlChE J. 65, 434–445. https://doi.org/10.1002/aic.16408.

Zarghami, S., Boukadi, F., Al-Wahaibi, Y., 2017. Diffusion of carbon dioxide in formation water as a result of CO2 enhanced oil recovery and CO2 sequestration. J. Petrol. Explor. Prod. Technol. 7, 161–168. https://doi.org/10.1007/s13202-016-0261-7.

Zhang, W., Wu, S., Ren, S., Zhang, L., Li, J., 2015. The modeling and experimental studies on the diffusion coefficient of CO2 in saline water. J. CO2 Utilization 11, 49–53. https://doi.org/10.1016/j.jcou.2014.12.009. The assessment of CO2 utilization technology in China.

Zhang, Y.P., Hyndman, C.L., Maini, B.B., 2000. Measurement of gas diffusivity in heavy oils. J. Pet. Sci. Eng. 25, 37–47. https://doi.org/10.1016/S0920-4105(99)00031-5.

Zhao, R., Xu, M., Yang, J., Fu, J.Y., Heng, M., Yue, X., 2018. Non-constant diffusion behavior for CO2 diffusion into brine: influence of density-driven convection. J. Solution Chem. 47, 1926–1941. https://doi.org/10.1007/s10953-018-0818-9.